Vision Research 75 (2012) 77–87

Contents lists available at SciVerse ScienceDirect

Vision Research

journal homepage: www.elsevier.com/locate/visres

Phenotypic expression of Bardet–Biedl syndrome in patients homozygous for the common M390R mutation in the *BBS1* gene

Kyle F. Cox [a], Natalie C. Kerr [a], Marina Kedrov [a], Darryl Nishimura [c], Barbara J. Jennings [a], Edwin M. Stone [b,d], Val C. Sheffield [c,d], Alessandro Iannaccone [a,*]

[a] University of Tennessee Health Science Center, Hamilton Eye Institute, Memphis, TN 38163, USA
[b] Univ. Iowa, Dept. of Ophthalmology and Visual Sciences, Iowa City, IA, USA
[c] Univ. Iowa, Dept. of Pediatrics, Division of Medical Genetics, Iowa City, IA, USA
[d] Howard Hughes Medical Institute, Iowa City, IA, USA

ARTICLE INFO

Article history:
Received 7 July 2012
Received in revised form 7 August 2012
Available online 24 August 2012

Keywords:
Bardet–Biedl syndrome
BBS1 gene
M390R mutation
Retinal degeneration
Phenotype–genotype correlation
Electroretinogram
Photoreceptors
Retinal nerve fiber layer
Visual fields
Retinal imaging

ABSTRACT

Purpose: To characterize the phenotype of Bardet–Biedl syndrome (BBS) patients homozygous for the *BBS1* M390R mutation.
Methods: Three patients [PT1, F, 27 years old (yo) at last examination, 14-year follow-up (F/U) PT2, F, 15-yo PT3, M, 15-yo, both 1-year F/U] underwent eye exams, Goldmann visual fields (GVFs), dark- (DA) and light-adapted (LA) electroretinograms (ERGs), spectral domain optical coherence tomography (SD-OCT) and fundus autofluorescence (FAF). Vision and systemic history were also collected.
Results: All patients had night blindness, hyperopic astigmatism, ptosis or mild blepharospasm, foot polydactyly, 5th finger clinodactyly, history of headaches, and variable, diet-responsive obesity. Two had asthma, PT1 was developmentally delayed, PT2 had Asperger-like symptoms, and PT3 had normal cognition. At age 14, acuity was 20/100 in PT1, who had nystagmus since age 2, 20/40 in PT2 and 20/30 in PT3. By 27 yo PT1 progressed to 20/320, by 15 yo PT2 was 20/60 and PT3 remained stable. PT1 had well preserved peripheral GVFs, with minimal progression over 10 years of F/U. PT2 and PT3 presented with ring scotomas and I4e < 5°. All patients had severe generalized visual sensitivity depression. ERGs were consistently recordable (also rod ERG in PT3 after 60 min DA), but progressed to non-recordable in PT1. Mixed DA ERGs exhibited electronegativity. In PT3, this was partly due to a bleaching effect during bright-flash DA averaging, partly to ON ≫ OFF LA response compromise. PT2 and 3 had, on SD-OCTs, generalized macular thinning, normal retinal lamination, and widespread photoreceptor outer/inner segment attenuation except foveally, and multiple rings of abnormal FAF configuring a complex bull's eye-pattern. PT1 had macular atrophy. All patients also had peripapillary nerve fiber layer thickening.
Conclusions: The observed phenotype matches very closely that reported in patients by Azari et al. (*IOVS* 2006) and in the *Bbs1*-M390R knock-in mouse model, and expands it to the characterization of important ERG response characteristics that provide insight in the pathogenesis of retinopathy in these patients. Our findings confirm the consistent pathogenicity of the *BBS1* M390R mutation.

1. Introduction

Bardet–Biedl syndrome (BBS) is a disorder characterized by retinal degeneration and multiple systemic manifestations including obesity, dystrophic extremities (polydactyly, syndactyly, brachydactyly and/or clinodactyly), abnormalities of the genitourinary tract including potentially life-threatening kidney dysfunction, secondary sexual development problems (hypogonadism more often in males, but virilism reported also in females), varying degrees of cognitive and behavioral abnormalities, and a host of other manifestations including hyposmia (Iannaccone, 2005; Iannaccone et al., 1997, 1999, 2005).

There are currently 17 identified genes which are involved in the development of BBS (https://sph.uth.tmc.edu/retnet/sum-dis.htm#B-diseases and Zhang, Yu, et al., 2012). To date, except for a tendency of BBS1 patients to exhibit on average a relatively milder phenotype than other forms of BBS (Azari et al., 2006; Daniels et al., 2012), no unique human genotype–phenotype association has emerged to permit differentiating BBS patients in subtypes depending on the associated genetic defect except for

* Corresponding author. Address: University of Tennessee Health Science Center, Hamilton Eye Institute, Department of Ophthalmology, 930 Madison Ave., Ste. 731, Memphis, TN 38163, USA. Fax: +1 901 448 5028.
E-mail address: aiannacc@uthsc.edu (A. Iannaccone).

0042-6989/$ - see front matter © 2012 Elsevier Ltd. All rights reserved.
http://dx.doi.org/10.1016/j.visres.2012.08.005

cases of non-syndromic RP linked to BBS gene mutations (Pretorius et al., 2010, 2011; Zhang, Nishimura, et al., 2012). This is likely due in part to the fact that most BBS genes, as are many others involved in retinal dystrophies, share the biological and disease-causing mechanistic basis of causing ciliary dysfunction (Loktev et al., 2008; Mykytyn & Sheffield, 2004; Seo et al., 2010; Zhang, Yu, et al., 2012). Although it has been proposed by some (Katsanis et al., 2001) that BBS may not routinely follow a Mendelian autosomal recessive inheritance pattern as traditionally believed, we and others have previously investigated the frequency of mutations other than the ones considered "primary" in BBS patients and could not find evidence to support the need for triallelism in BBS (Mykytyn et al., 2003). The consistent phenotypic effects observed in mice whose hortolog genes have been knocked out or that, subsequently, had specific mutations like the *BBS1* M390R one knocked-in (Davis et al., 2007; Mykytyn et al., 2004; Swiderski et al., 2007; Zhang, Nishimura, et al., 2012), confirms that BBS remains a Mendelian autosomal recessive disease. However, the aforementioned biological and disease-causing mechanistic overlap among many BBS genes at the ciliary basal body makes the possibility of epistatic effects exerted on the main phenotypic determinants by secondary mutations quite plausible and, surely in some cases, highly likely (Badano et al., 2003).

BBS has been a key focus of the work of our group for nearly two decades. Despite the wide genetic heterogeneity of BBS and the elusiveness of genotype–phenotype correlations, it has been reported that approximately 80% of the Caucasian patients with BBS1 carry the M390R mutation within the *BBS1* gene, which is also the most common gene involved in BBS (Mykytyn et al., 2002). The M390R mutation alone accounts for approximately 27% of all cases of BBS (Sheffield, Nishimura, & Stone, 2012, unpublished observation). Therefore, there is much value in understanding the phenotypic effects in humans of this specific mutation for the BBS research field. In recent years, mouse models for BBS have been developed, including one in which the *Bbs1* M390R mutation has been knocked in (Davis et al., 2007), and preclinical gene transfer and pharmacologic therapies have shown a great deal of potential for achieving successful treatment of BBS (Drack et al., 2011; Simons et al., 2011). Among these, and of particular relevance to this manuscript, was the benefit observed with TUDCA supplementation in the aforementioned *Bbs1-M390R* knock-in mice on both the retinal and the obesity phenotype (Drack et al., 2011). To the best of our knowledge, only one previous paper has documented in detail the clinical, microanatomical, and functional phenotypic expression of BBS1 patients (Azari et al., 2006).

The growing understanding of BBS pathophysiology, the prospect of treatments becoming potentially available in the near future, and the availability of three patients homozygous for the common M390R *BBS1* mutation prompted us to conduct a retrospective investigation of their phenotypic presentation. Herein we will illustrate how the retinal phenotype linked to homozygosity for the M390R *BBS1* mutation exhibits remarkable homogeneity with the previously reported one (Azari et al., 2006), while displaying variability at the systemic end. We will provide additional evidence for impaired post-receptoral function consistently affecting the retinas of these patients, as well as evidence for defective visual pigment recycling. Our data both corroborate previous findings (Azari et al., 2006) and expand our understanding of the phenotypic expression of BBS linked to the common M390R *BBS1* mutation. Furthermore, our data offered us the possibility to draw a parallel with the retinal phenotype exhibited by *Bbs1-M390R* knock-in mice, showing how this model reproduces closely human disease expression and allowing us to gain insight in the pathogenesis of human retinal disease.

2. Materials and methods

2.1. Subjects

Three previously unreported patients with BBS were included in this retrospective investigation. Basic demographics of the three patients are reported in Table 1. The genotype was ascertained via molecular genetic diagnostic testing performed by the Carver Lab at University of Iowa. After obtaining informed consent for testing, genomic DNA was extracted from whole blood samples collected from the probands and their parents and PCR-amplified according to standard procedures. Probands were tested with the targeted BBS diagnostic screening panel currently offered by the Carver Lab, aimed at determining if they carried either the common *BBS1* Met390Arg (M390R) or the common *BBS10* Leu90 ins 1 T mutations. All three patients were found to be homozygous for the common *BBS1* M390R mutation, and parental sample analyses confirmed that each allele was carried in the heterozygous state by each asymptomatic parent.

Each patient was interviewed with a standardized questionnaire to collect detailed information of type, age of onset, severity and progressive nature of visual symptoms. Systemic manifestations were also documented in detail by history as well as by physical observation and examination.

All subjects underwent clinical ocular examinations including determination of best corrected visual acuity with standard ETDRS charts, assessment of ocular adnexa and motility, anterior and posterior segment slit lamp examination, imaging studies inclusive of color fundus photography and spectral domain optical coherence tomography (SD-OCT) of the macula and disk (see Supplemental Methods section for additional information). High-resolution, 30° cross sectional SD-OCT images of the macula intersecting the foveal dip were obtained from PT2 and PT3. At the latest examination, images were also obtained with enhanced depth imaging (EDI) methodology, as described by Spaide, Koizumi, and Pozzoni (2008). PT2 and PT3 had retinal nerve fiber layer (RNFL) thickness measured with the standard optic disk cube protocol of the Cirrus SD-OCT (Zeiss Meditec, Dublin, CA). In addition, cross sectional SD-OCT images were obtained for the optic nerve of PT3 along with custom RNFL thickness measurements (Supplemental Methods and Figure). Fundus autofluorescence (FAF) images could also be obtained on PT3 (Supplemental Methods). PT1 and PT2 experienced too much light aversion to undergo FAF with this methodology. PT1 experienced also an excessive amount of nystagmus and had inadequate fixation to permit obtaining reliable SD-OCT scans of sufficient quality for further analysis.

Visual function studies included Goldmann visual fields (GVFs), full-field flash electroretinograms (ERGs) and, when possible, automated monochromatic light- and dark-adapted perimetry. GVFs performed with a minimum of two targets (V4e and I4e) as previously reported (Iannaccone et al., 2004, 2006, 2008). See Supplemental Methods for specific details on GVF field size calculations. The calculated net field area was compared to our published normative data (Iannaccone et al., 2004), and expressed as percent of the lowest limit of these normal ranges. Flash ERGs were performed in all subjects with an Espion2 and, more recently, an Espion3 system (Diagnosys LLC, Lowell, MA, USA) at baseline and at follow-up examinations with monopolar corneal electrodes (ERG-Jet, Universo Plastique AS, Grenchen, Switzerland) as previously reported (Iannaccone et al., 2006). Responses were recorded at various points in time on PT1 during the 15-year follow-up period, initially also with a Nicolet Spirit system (Viasys Nicolet Biomedical, Madison, WI, USA). Additional ERG methodology details are provided in the Supplemental Methods section. The amplitude (in μV) of the a- and b-waves were compared to the

Table 1
Clinical characteristics of our BBS1 patients homozygous for the M390R mutation.

Characteristic	Patient					
	PT1		PT2		PT3	
Age (first/last examination)	12/27 yo		14/15 yo		14/15 yo	
Gender	F		F		M	
Symptoms of onset (age)	Nystagmus (2 yo)		Reduced VA (3 yo)		Peripheral vision loss (1 yo)	
	Night blindness (3 yo)		Night blindness (7 yo)		Night blindness (5 yo)	
Best corrected visual acuity	OD	OS	OD	OS	OD	OS
– First examination	20/60	20/80	$20/50^{+2}$	$20/32^{-2}$	20/50	20/40
– Last examination	20/320	20/400	$20/60^{+1}$	$20/40^{+1}$	20/60	20/80
Refraction	$+1.50 + 3.25 \times 105$	$+1.00 + 3.00 \times 085$	$+1.75 + 2.00 \times 075$	$+0.50 + 3.50 \times 110$	$+2.00 - 1.25 \times 180$	$+1.00 - 1.50 \times 180$
Eyelids	Dermatochalasis mild ptosis	Dermatochalasis moderate ptosis	Mild blepharospasm	Mild blepharospasm	Mild ptosis	Mild ptosis
Post. subcapsular cataract	Axial, dense	Axial, dense	None	None	None	None
Goldmann visual field (age)	18/25 yo		14/15 yo		14/15 yo	
– First examination (V4e/I4e)	69%, 0%	75%, 0%	51%, <1%	47%, <1%	84%, <0.1%	100%, <0.1%
– Last examination (V4e/I4e)	67%, 0%	64%, 0%	55%, 0%	50%, 0%	89%, <0.1%	91%, <0.1%
Flash ERGs (last examination)						
– DA rod 0.08 cd s/m^2	N/R	N/R	N/R	N/R	N/R 30', 25% 60'	N/R 30', 28% 60'
– DA mixed 2.1, 10.0 cd s/m^2	N/R	N/R	a-w: 7%, 13% b-w: 5%, 3%[a]	a-w: 6%, 5% b-w: 5%, 5%[a]	a-w: 34%, 23% b-w: 34%, 16%[a]	a-w: 27%, 32% b-w: 34%, 16%[a]
– LA cone 2.1, 10.0 cd s/m^2	N/R	N/R	b-w: 22%, 28%	b-w: 15%, 22%	b-w: 21%[a], 36%	b-w: 18%[a], 28%
– LA flicker 2.1, 10.0 cd s/m^2	N/R	N/R	15%, 15%	12%, 15%	26%, 38%	21%, 35%

Our normative data range (95th confidence interval around the mean) for the 10 (+1.0 log) cd s/m^2 stimuli amplitudes and timing are: DA mixed a-wave: 250–387 μV, 11.0–15.3 ms; DA mixed b-wave: 346–571 μV, 38.3–51.3 ms; LA cone b-wave 96–196 μV, 27.0–34.8 ms; LA flicker peak: 104–218 μV, 28.2–33.4 ms.
[a] Electronegative ERG b-wave.

lowest amplitude of the normal range for our lab (2.5th percentile) and expressed as percentages of these limits. Our normative data for these stimulus conditions (95% confidence intervals around the mean) have been previously published (Iannaccone et al., 2006) except for the 10(1.0 log) cd s/m^2 stimuli, which are reported herein.

In addition to these standard recordings, because of suspicion of a bleaching effect causes by the bright flashes in the DA state suggestive of defective recycling of the visual pigments (see below, Section 3), rod-driven flash ERGs were also obtained in PT3 after prolonged DA (60 min). To ascertain further the relative degree of impairment of post-receptoral responses originating from ON- and OFF-cone bipolar cells, photopic ON–OFF ERGs were also recorded in PT3 in response to 125-ms square-wave stimuli (Khan et al., 2001; Sieving, 1993; Sieving, Murayama, & Naarendorp, 1994) alternating at a 4.5-Hz frequency and to rapid-ON and rapid-OFF, 8.5-Hz saw-tooth stimuli (Alexander, Barnes, & Fishman, 2001), both presented on a bright LA background of 150 cd/m^2. PT2 was unable to undergo ON–OFF photopic ERGs due to excessive light aversion. The responses of PT1 were too small to permit this additional level of investigation.

3. Results

Some of the salient demographic, clinical and functional findings for our three BBS1 patients homozygous for the M390R mutation are summarized in Table 1. In brief, all patients experienced night blindness at onset, which developed between 3 and 7 years of age. All three subjects also had congenital polydactyly, history of headaches and variable, diet-responsive obesity. Further details about the phenotypic findings observed in each of these three subjects are described in the following sections and are illustrated in Figs. 1–4. Once evaluated at baseline, each patient was counseled to the potential benefits and limitations of vitamin A palmitate, lutein, and DHA supplementation in RP, with the caveat that no BBS patient and no children had been included in the trials that reported reduced disease progression in association with these supplements (Berson et al., 1993, 2004a, 2004b, 2011). All subjects took, at least in part (see below), these supplements. Therefore, follow-up data has to be intended not as the natural history of disease progression in these three patients, but the changes experienced during such dietary supplementations.

3.1. Patient 1 (PT1)

PT1 was first seen at the age of 12 years old. In addition to early onset night blindness, PT1 also had history of nystagmus noted since age 2. She exhibited the most severe manifestations of the three patients, both systemically and ophthalmically. Systemic features included marked developmental delay, truncal obesity (Fig. 1A) and post-surgical polydactyly with clinodactyly of the 5th finger (Fig. 1C). She took 15,000 IUs of vitamin A palmitate supplements daily from age 12 until present, followed by the addition of lutein 20 mg/day as of age 18 and fish oil supplements containing an equivalent daily DHA dose of 1000 mg since age 23. No liver function or other systemic problems were reported during this period of supplementation.

Upon eye examination, visual acuity was 20/60 OD and 20/80 OS at baseline and was 20/320 OD and 20/400 OS at the latest exam, showing a progressive decrease over the 15-year follow-up (Table 1), only in part explained by the development of bilateral axial dense subcapsular cataracts. She also had bilateral superior eyelid dermatochalasis with mild left ptosis (Fig. 1B). Fundus examination demonstrated central macular atrophy noted at age 18 (Fig. 2A) which progressed to an additional ring of bull's eye maculopathy at age 25 (Fig. 2B). Progressive RPE atrophy at the arcades and mid-periphery alongside modest bone spicule-like intraretinal deposits were also apparent (Fig. 2A and B). Despite the overall severity of her macular disease and its progressive nature, by GVF criteria, PT1 had fairly well preserved peripheral visual fields limits, though markedly depressed in peripheral sensitivity. The superior visual field defect may have resulted from both her blepharochalasis and ptosis (the patient could not tolerate eyelid taping) and greater severity of inferior retinal pathology. There

Fig. 1. Systemic and external manifestations. PT1: (A) marked obesity with a prevailing truncal distribution (BMI: 33.7). (B) Dermatochalasis of both upper eyelids and mild asymmetric ptosis (OS > OD). (C) Clinodactyly of the 5th finger associated with skin scarring following surgical removal of supernumerary 6th finger of the right hand (arrow). PT2: (D) sequelae of surgical correction of syndactyly and polydactyly of the left hand, and clinodactyly of the 5th finger (arrows). (E) Small lateral scars following surgical removal of bilateral polydactyly of the feet (arrows), relative brachydactyly of the 5th toes, and mild leg hirsutism (asterisk). PT3: Sequelae of surgical correction of polydactyly of the left (F) and right (G) foot. (H) Mild clinodactyly of the 5th finger.

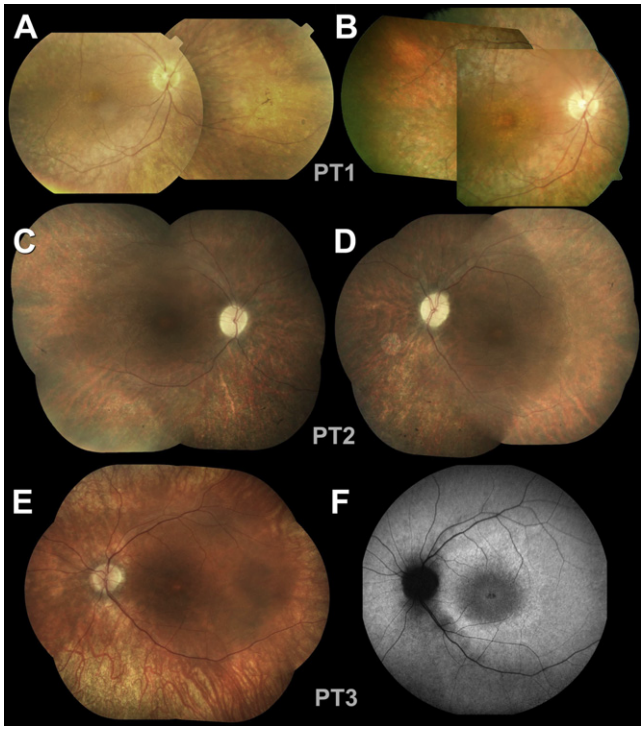

Fig. 2. En-face imaging findings. PT1: (A) fundus composite of OD at age 18 showing waxy pallor of the disk, vascular attenuation, macular RPE atrophy, diffuse mid-peripheral RPE dropout with partial choroidal visualization, and rare mid-peripheral intraretinal pigmentary deposit (inferonasal quadrant). (B) Fundus composite of OD at age 25 showing increase in macular RPE atrophy, disk pallor and RPE dropout also at the arcades. A faint bull's eye pattern of perifoveal RPE dropout can also be appreciated. PT2: Fundus composite of OD (C) and OS (D) at age 15 presenting with full, waxy pale disks, vascular attenuation, macular RPE dropout, diffuse mid-peripheral RPE dropout with choroidal visualization in the inferior quadrants, where also a few intraretinal punctate pigmentary deposits can be seen. In OS, a nummular area of discrete RPE atrophy can also be seen inferonasal to the disk. PT3: (E) fundus composite of OS at age 15 showing a full, mildly hyperemic disk surrounded by a pale halo, focal macular RPE dropout, mid-peripheral RPE loss and coarse mottling both superiorly and inferiorly with pronounced choroidal visualization in the inferior quadrants. No intraretinal pigment deposits are apparent. (F) Fundus autofluorescence (FAF) at age 15, showing (a) loss of autofluorescence (AF) around the disk consistent with peripapillary RPE loss and (b) a complex bull's eye-like pattern in the macular region characterized by multiple concentric rings of abnormal AF: an ill-defined, irregularly shaped ring of hyper-AF around the macula surrounds a wide parafoveal halo of hypo-AF within which there is a tight perifoveal ring of near-normal AF, surrounding a focal foveal area of marked hypo-AF, consistent with the subfoveal RPE dropout noted clinically.

was essentially no change in GVF size or quality after a 7-year follow-up period (Fig. 3A, B and Table 1). However, consistent with increasing macular disease progression, slight contraction of the central area of I4e detection was seen. ERGs were first performed at age 15 and demonstrated marked delayed responses, albeit still clearly recordable (Fig. 4). At age 17, transient electronegativity in the mixed ERG responses was observed (not shown) and by age 25, ERGs became non-recordable. FAF, SD-OCTs and ON–OFF LA ERGs could not be performed on this patient.

3.2. Patient 2 (PT2)

PT2 was first seen at the age of 14 and has 1 year of follow-up data. Night blindness was first noted at 7 years of age. Systemic features included diet-responsive truncal obesity (latest BMI: 27.4, before diet and exercise: 34), syndactyly and polydactyly of the left hand (surgically corrected) and clinodactyly of the 5th digit of the left hand (Fig. 1D). She also had bilateral polydactyly of the feet (surgically corrected), relative brachydactyly of small toes, and mild hirsutism of both legs (Fig. 1E). After the initial examination, she started taking 15,000 IUs/day of vitamin A palmitate, lutein 20 mg/day, and fish oil supplements containing an equivalent daily DHA dose of 1000 mg. No liver function or other systemic problems have been reported during this short period of supplementation.

Visual acuity was $20/50^{+2}$ OD and $20/32^{-2}$ OS at baseline examination and declined at the last two examinations to $20/60^{+1}$ OD [a 6-letter, or 0.12 logMAR change, which is significant for undilated acuity measurements in RP patients (Grover et al., 1997)] and $20/40^{+1}$ OS (Table 1). The lens was clear bilaterally and fundus examination demonstrated (Fig. 2C and D) macular and diffuse peripheral RPE dropout bilaterally, the latter more pronounced inferiorly with a coarse moth-eaten appearance and, in OS, a discrete area of nummular RPE atrophy infero-nasal to the disk, markedly attenuated retinal vasculature, and waxy pale, full disks. Only a few intraretinal pigment deposits, mainly punctate in appearance, were seen in the inferior quadrants. These clinical findings did not change during follow-up. Macular and RNFL SD-OCT (Fig. 5A and B) showed generalized thinning of the neural retina with well-preserved retinal lamination, markedly attenuated photoreceptor outer/inner segment (PR-OS/IS) junction and of the outer nuclear layer (ONL) with relative foveal sparing, and *thickened* rather than thinned RNFL by Cirrus SD-OCT criteria. FAFs could not be performed reliably on this patient secondary to light aversion.

GVFs were characterized by overall superior > inferior visual field loss and full, absolute ring scotomas with a large island of peripheral vision in the inferior farthest hemifield (Fig. 3C). Over the 1-year follow up (Fig. 3D), GVFs showed loss of central sensitivity from baseline (I4e no longer detected, central isopter delimited

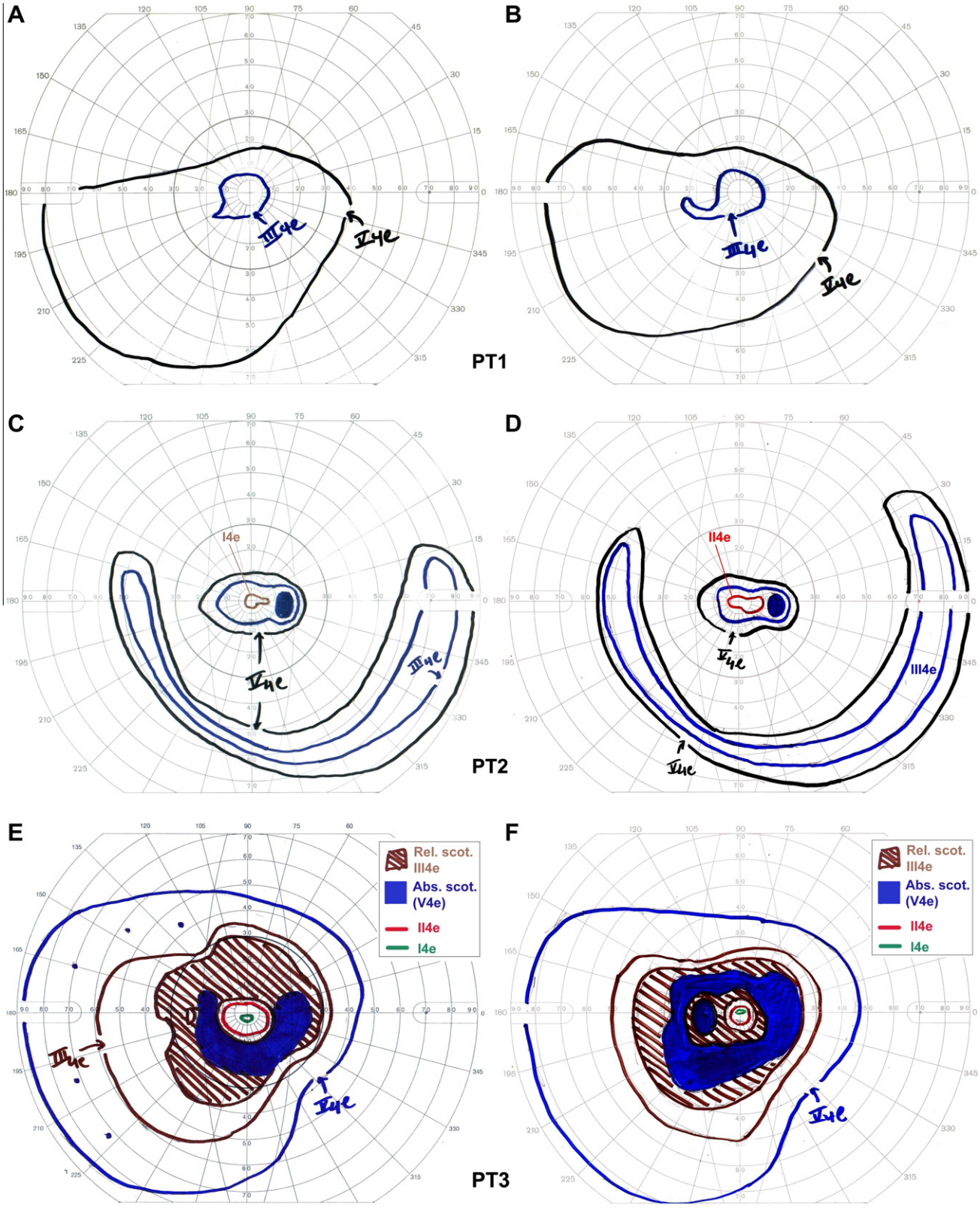

Fig. 3. Patterns of Goldmann visual field loss. PT1: Representative GVFs from OS at age 18 (A) and at age 25 (B) demonstrate superior > inferior field loss, generalized sensitivity depression, and essentially neither qualitative nor quantitative change over time. No scotomatous areas could be detected in the mid-periphery (not shown). PT2: Representative GVFs from OD at age 14 (C) and age 15 (D): similar to PT1, there is overall greater superior visual field loss; however, the pattern of disease expression differs, with absolute mid-peripheral ring scotomas separating the central field from a large island of peripheral vision in the farthest part of the inferior hemifield. During the short-term follow-up period, there was no significant change peripherally, but there was evidence of loss of central sensitivity from baseline (I4e no longer detected at age 15, only the II4e target could be detected centrally). PT3: Representative GVFs from OS at baseline (age 14, E) and at age 15 (F) demonstrate overall preservation of the peripheral limits to the V4e target, pericentral scotomas of variable density at baseline, progressing to an absolute ring scotoma in only 1 year. This change was associated also with short-term loss of both peripheral (III4e) and central (I4e) sensitivity, and with a tightening of the pericentral scotoma around fixation. These findings parallel closely the ophthalmoscopy and FAF findings illustrated in Fig. 2.

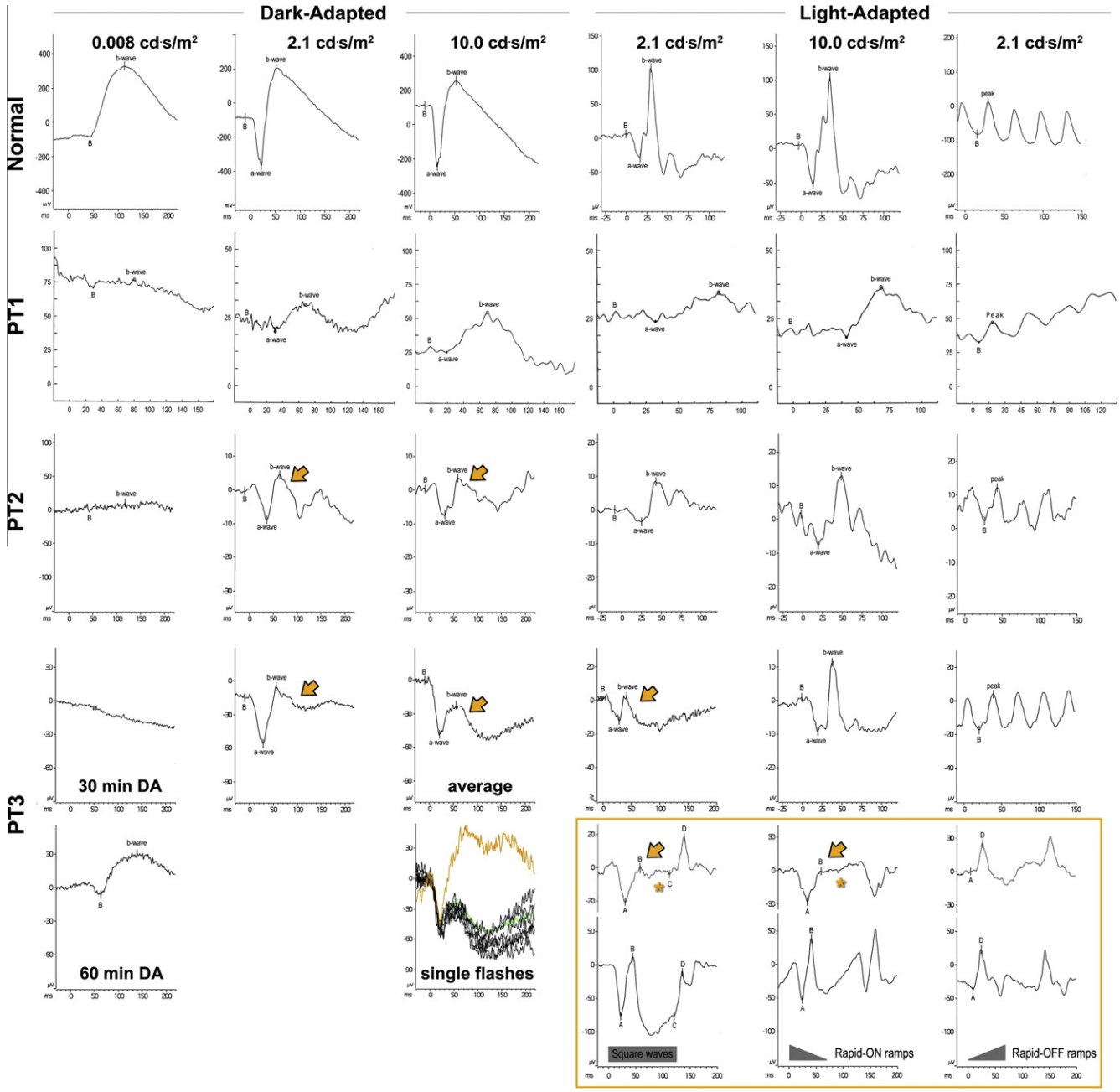

Fig. 4. Standard and custom baseline dark- (DA) and light-adapted (LA) electroretinogram (ERG) responses. Top row, normal example of a series of standard responses for our lab, including DA rod-driven (0.008 cd s/m^2, or −2.1 log cd s/m^2), DA mixed rod-cone [2.1(+0.32 log) and 10(+1.0 log) cd s/m^2], LA cone transient [2.1(+0.32 log) and 10(+1.0 log) cd s/m^2], and cone flicker [2.1(+0.32 log) cd s/m^2] ERG responses. Second row, PT1: ERGs at age 15: DA rod-driven and mixed rod-cone ERGs were markedly diminished and delayed but still recordable. LA cone-driven transient and flicker ERGs were also markedly diminished and extremely delayed but still recordable. No electronegativity was observed at this stage, but this feature became apparent in the mixed response subsequently (not shown), followed by diminution of the responses below the recordable threshold (not shown). Third row, PT2: DA rod-driven ERGs are barely detectable. DA mixed rod-cone ERGs were clearly measurable, though diminished and delayed, and they showed disproportionate b-wave reduction (arrows) compared to the a-wave. LA Cone-driven transient and flicker showed delayed and decreased amplitude responses with relatively normal b-wave shape. However, the a-wave was square-shaped, and there was selective reduction of the b-wave response (ON-mediated) compared to the ensuing d-wave (OFF-mediated), indicating ON > OFF post-receptoral compromise. Fourth and fifth row, PT3: Standard 30-min DA rod-driven ERGs were non-recordable, whereas after 60-min DA they were delayed yet clearly recordable. The averaged DA mixed responses showed progressively more b-wave truncation with increasing flash intensity. Breaking down the 10(+1.0 log) cd s/m^2 response to single flashes, the response to the first flash (in orange) exhibited no electronegativity, whereas all others did. Besides being delayed and reduced in amplitude, also LA responses were electronegative in response to the 2.1(+0.32 log) cd s/m^2 stimulus, which was not due to a phenomenon similar to that seen for DA ones (not shown). Therefore (inset within the bottom row in the LA section), ON–OFF ERGs were recorded from PT3 (top row within the inset). Compared to a normal example (bottom row of responses within the inset), responses showed ON-driven b-wave electronegativity (arrows) and abnormal plateaus following the b-wave (asterisk) to both square wave and rapid-ON ramp stimuli. Unlike these, responses to both square wave and rapid-OFF ramp stimuli were delayed and mildly reduced but otherwise overall normal in shape.

now only with the II4e target) but only modest changes (trending for the better) in terms of peripheral field size. The DA rod-driven and mixed rod-cone ERGs and LA cone-driven ERGs were all markedly reduced and markedly delayed but readily recordable. Moreover, the mixed ERG response showed disproportionate b > a-wave reduction bilaterally (see arrows, Fig. 4). ON–OFF LA ERGs could not be performed reliably on this patient secondary to light aversion.

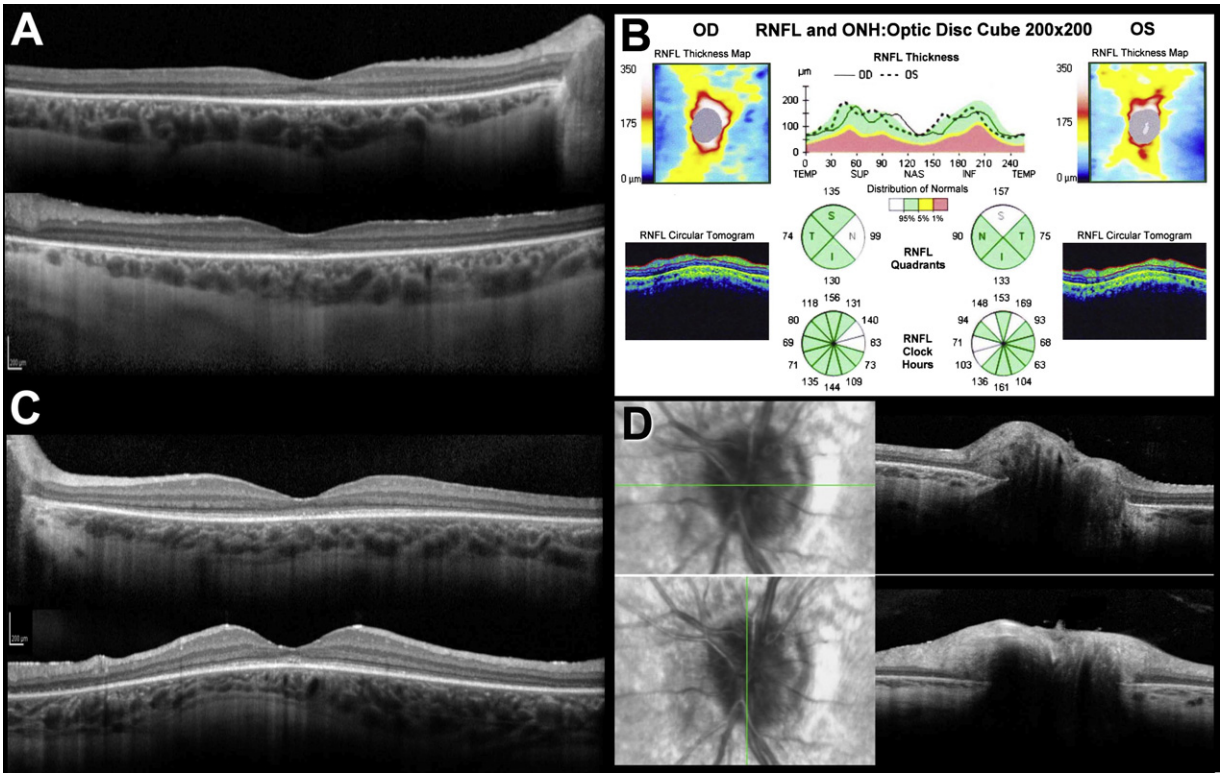

Fig. 5. Spectral domain optical coherence tomography (SD-OCT) findings. PT2: Transfoveal horizontal Spectralis EDI SD-OCTs (A) show generalized thinning of the neural retina, markedly attenuated photoreceptor outer/inner segment (PR-OS/IS) junction with a good residue only in the foveal region, yet well defined retinal lamination in both eyes, as well as an epiretinal membrane characterized by retinal surface wrinkling in OD > OS; (B) Cirrus peripapillary RNFL SD-OCT showed RNFL thickening in several quadrants (pie slices labeled in white) and normal RNFL thickness elsewhere (green pie slices) in both eyes. PT3: Horizontal and vertical transfoveal Spectralis EDI SD-OCTs (C) of the left eye show mildly thinned neural retina, moderately attenuated PR-OS/IS junction in the peripheral portions of the scans but good preservation thereof throughout the remainder of the scan, except that the foveal residue presents significant irregularities; retinal lamination is very well preserved, and modest and focal thickening of the vitreoretinal interface can be also appreciated. Horizontal and vertical transpapillary Spectralis SD-OCTs of the same eye (D) show swollen disk devoid of physiologic cupping, thickened RNFL, and the incidental finding of a small epipapillary residue of the hyaloid vasculature and some epipapillary vitreal debris. Please refer to Supplemental Figure for further details about the RNFL findings in PT3. Findings were comparable in the right eye (not shown). (For interpretation of the references to color in this figure legend, the reader is referred to the web version of this article.)

3.3. Patient 3 (PT3)

PT3 was first seen at the age of 14 and again at the age of 15. Night blindness was experienced by this patient at 5 years of age. Systemic features included diet-responsive obesity (BMI on diet and exercise: 28.2, latest BMI after discontinuation of regimen: 29.4), bilateral polydactyly of the feet which was surgically corrected (Fig. 1F and G, arrows) and clinodactyly of the 5th digit of the right hand (Fig. 1H). After the initial examination, he started taking 15,000 IUs/day of vitamin A palmitate, lutein 20 mg/day, and fish oil supplements containing an equivalent daily DHA dose of 1000 mg. Shortly after beginning supplementation, PT3 experienced significant worsening of his preexisting history of headaches. Serial disk SD-OCTs were also obtained during this period with both the Cirrus and the Spectralis instruments, and custom RNFL thickness measurements were performed at several locations around the disk on SD-OCT scans intersecting the optic nerve head (see Supplemental Figure). The standard circular scan of the Cirrus SD-OCT failed to reveal RNFL thickening in this patient. However, when compared to measurements at matching locations from scans obtained from a normal subject, custom RNFL thickness measurements made on the Spectralis scans immediately around the lamina cribrosa opening demonstrated a significant difference between the thickness of the RNFL in PT3 compared to normal on both the vertical and horizontal axis ($p = 0.007$ and 0.03, respectively, Student's paired two-tailed T-test). Out of concern for a possible adverse effect of vitamin A on intracranial pressure, this supplement was discontinued, which led to a resolution of the complaint. No other side effects were reported during the 1-year follow-up while on the other supplements. Serial Spectralis SD-OCTs showed a restoration of the physiological disk cupping after vitamin A discontinuation, which suggested that, in this patient, the use of vitamin A may have contributed to an increase in intracranial pressure and disk swelling, but the increased RNFL thickness surrounding the disk persisted at subsequent examinations (see Supplemental Figure), consistent with RNFL thickening also in this patient being independent of vitamin A use.

Visual acuity was 20/50 OD and 20/40 OS at baseline examination and 20/60 OD and 20/80 OS at last examination. The lens was clear bilaterally and fundus examination demonstrated macular and peripheral RPE atrophy, leading to visualization of the underlying choroidal vasculature (Fig. 2E). FAF revealed multiple, macular bull's eye-like and peripheral rings of increased and decreased AF with superior and inferior RPE loss (Fig. 2F). Macular and disk SD-OCT showed thinned neural retina, markedly attenuated PR-OS/IS junction with fair foveal residue, preserved retinal lamination, and swollen disks with thickened RNFL (Fig. 5C and D). GVFs at baseline showed marked depression in peripheral sensitivity yet essentially full-size fields with pericentral scotomas that progressed to an absolute ring scotoma, tighter around fixation, after the 1-year follow-up (Fig. 3D and E). No field expanse loss was observed over this period, but central sensitivity appeared reduced compared to baseline. The bottom two rows of Fig. 4 illustrate the ERG responses of PT3, who had the best preserved responses

of all three subjects. The DA rod-driven ERG was non-recordable after a standard period of 30 min of dark adaptation. Mixed DA rod-cone responses demonstrated electronegativity resulting from b-wave depression that increased with brighter flash intensities in the averaged responses. However, unaveraged single-flash responses to 10.0 cd s/m^2 flashes showed a large b-wave in response to the first flash (Fig. 4, bottom row, orange trace), followed by a series of responses with much smaller b-waves. Except for a modestly faster b-wave peak time to ensuing flashes, this phenomenon in our hands is never observed in normal subjects, but is closely reminiscent of what patients with fundus albipunctatus (FA) and retinitis punctata albescens (RPA) can show (Fishman et al., 2004; Iannaccone et al., 2007). This finding raised the suspicion of a bleaching effect caused by the bright flashes in the DA state, suggestive of defective recycling of the visual pigments. To test this hypothesis, rod-driven flash ERGs were also obtained in PT3 after prolonged dark adaptation (60 min, Fig. 4, bottom row, left-hand column). Consistent with our suspicion, a rod-driven response could be clearly recorded after 60 min in the dark, albeit markedly reduced. The LA cone ERGs were markedly reduced in amplitude and delayed. The transient LA cone ERG responses demonstrated also electronegativity. This finding, alongside the electronegativity of ERG responses observed also in PT2 and, transiently, in PT1 suggested that BBS1 patients with the M390R mutation may experience abnormal post-receptoral intraretinal signal processing. To ascertain further the relative degree of impairment of post-receptoral responses originating from ON- and OFF-cone bipolar cells, photopic ON–OFF ERGs were recorded (Fig. 4, top series of responses in the orange inset). ON–OFF LA ERGs exhibited several abnormalities. The ON-driven b-wave to both square-wave stimuli and saw-tooth was markedly depressed and delayed (arrows) compared to normal (Fig. 4, bottom series of responses in the orange inset). These waveforms were followed by abnormal plateaus (asterisks) that are not usually observed in normal responses. Unlike ON responses, OFF responses were somewhat reduced in amplitude but were for the most part normal in shape and timing, indicating that ON-bipolar cell activation was preeminently compromised.

4. Discussion

Phenotypic manifestations of BBS1 (*M390R* genotype) have become increasingly well documented in recent years (Azari et al., 2006; Deveault et al., 2011). Our investigation confirmed many of the ophthalmic, and specifically retinal, clinical and functional features exhibited by BBS1 patients, found consistent, confirmatory evidence for an effect of this genotype of post-receptoral retinal function, and revealed also novel findings.

From a systemic standpoint, all patients had abnormal extremities (foot polydactyly and 5th-finger clinodactyly was seen in all), history of headaches, and variable obesity, which was diet-responsive in PT2 and PT3. These findings are similar to previous reports on BBS1 patients, with digital anomalies and obesity being the most common systemic features noted also by others (Azari et al., 2006; Deveault et al., 2011). PT1 and PT3 had asthma, and PT2 also had hirsutism. Asthma is not a feature commonly considered typical of BBS. However, asthma too has been reported consistently more often in BBS1 (~38%) than in other BBS subtypes (Beales et al., 1997; Deveault et al., 2011). As the role of the BBS genes in ciliary function, including that of the respiratory trait, becomes increasingly understood (Shah et al., 2008), asthma and other respiratory manifestations may become an increasingly appreciated manifestation of BBS, and of BBS1 in particular.

Only PT1 had documented urinary tract problems (incontinence and recurrent infections) but none had evidence of kidney abnormalities, which are instead considered fairly typical for BBS (Anadoliiska & Roussinov, 1993; Campo & Aaberg, 1982; Churchill, McManamon, & Hurley, 1981; Green et al., 1989; Hurley et al., 1975; Iannaccone et al., 1997; O'Dea et al., 1996; Ozer et al., 1995; Perez Perez & Barrio, 1998). The proportion of our patients with urinary tract problems (one in three cases) is comparable to the prevalence noted by Deveault et al. (2011), who found ultrasonography-demonstrated kidney abnormalities in 38% of their BBS1 patients, and by Azari et al. (2006), who reported renal problems in 30% of their BBS1 patients. This prevalence is lower than what Deveault et al. (2011) observed in their BBS patient population as a whole (53%). Notwithstanding the lower frequency of kidney changes noted in BBS1, the possibility that renal dysfunction may develop at later stages of the disease remains, and patients should still be monitored longitudinally for signs of this problem that carries such significant morbidity risk for BBS patients (O'Dea et al., 1996).

The cognitive and behavioral status of our three patients varied widely. PT1 was overtly developmentally delayed, PT2 had Asperger-like symptoms, and PT3 had apparently normal cognition. This wide range of phenotypic expression at the cognitive end has been previously noted in BBS (Barnett et al., 2002; Iannaccone et al., 1997; Jacobson, Borruat, & Apathy, 1990) and has more recently been confirmed also for BBS1 (Azari et al., 2006; Deveault et al., 2011).

Clinical ocular findings varied in severity, but were quite consistent among the three patients and, for the most part, with previous reports. Night blindness was a consistent finding at an early age in all subjects. All of our BBS1 patients already had decreased visual acuity at their baseline examinations. The severity of this visual acuity reduction spanned over a wide range, as noted by Azari et al. (2006) and Daniels et al. (2012). In addition, all patients experienced further acuity deterioration over time, even in the course of the short follow-up of PT2 and PT3. Progressively deteriorating visual acuities have been consistently reported in BBS (Fulton, Hansen, & Glynn, 1993; Leys et al., 1988; Riise et al., 1996). Consistent with these early reports, Deveault et al. (2011) reported progressive visual loss in the majority of patients regardless of genotype. Therefore, while it has been suggested that BBS1 patients may have better visual acuity than other forms of BBS at presentation (Daniels et al., 2012), the potential for significant progressive acuity loss in BBS1 patients homozygous for the M390R mutation remains.

Ophthalmoscopy consistently showed attenuation of the retinal vasculature, RPE dropout both in the macular region and peripherally, and poverty of intraretinal pigmentary deposits in all patients, even in PT1 who was followed up for an extensive period of time. The finding of RP sine pigmento at presentation in BBS has been previously reported as the most common expression of retinopathy in a molecularly uncharacterized series of BBS patients (Iannaccone et al., 1997). Intraretinal pigmentary deposits as seen in RP tend to develop later on in the life of BBS patients (Iannaccone et al., 1997; Riise et al., 1996), which can make the recognition of the syndromic retinopathy phenotype and the correct formulation of the diagnosis of BBS at referral challenging (see, e.g., cases P3, P7 and P10 in the series by Azari et al., 2006).

Imaging studies were very informative. Macular OCT findings (Fig. 5) demonstrated normal to near normal central retinal thickness in PT3 and overall thinning of the neural macular retina in PT2. In both patients, outside of the centermost region, there was overt loss of the photoreceptor layers (both of the ONL and the PR-OS/IS boundary) but very good preservation of retinal lamination. The extent of overall photoreceptor compromise by OCT criteria was much more severe in PT2 than in PT3, highlighting the aforementioned variability in disease severity observed among these three patients. Foveal photoreceptors were still fairly well preserved also in PT2, although the PR-OS/IS boundary was clearly

irregular foveally in both patients. These findings are consistent with what was observed in previous reports (Azari et al., 2006; Deveault et al., 2011). FAF also revealed in PT3 that, while photoreceptors appear still in fairly good health centrally by OCT criteria, significant bull's eye-shaped loss of perifoveal FAF is already present at this stage, and that a ring of pericentral increase in FAF is also present outside the area of FAF loss. In all patients, RPE diffuse and, at times, discrete dropout was apparent also by ophthalmoscopic criteria (Fig. 2). Taken together, these findings underscore a tendency for BBS1 linked to the M390R mutation to affect early and significantly the macular region and to be associated with RPE loss. The findings of macular atrophic changes and progressive visual acuity loss have been previously reported in BBS1 patients (Azari et al., 2006; Deveault et al., 2011). Our longitudinal observations suggest progressive loss in central visual function also in the relatively short term. This may be due to progressive photoreceptor disease, as a ciliopathy would predict and as our photographic and SD-OCT data suggest (Figs. 2 and 5). However, the finding of thickened RNFL may indicate that RGC/optic nerve pathology may also contribute over time to the visual acuity deficit of these patients, as we previously reported (Iannaccone et al., 1997).

At a time when genes for BBS had yet to be cloned and SD-OCT technology had yet to become widely available, we reported that, compared to non-syndromic recessive RP, optic nerve involvement represented by disk pallor and overt atrophy ascertained clinically is common in BBS (Iannaccone et al., 1997), a finding which appeared to correlate better with the degree of visual acuity loss in BBS than macular retinal changes. In their study of BBS1 patients, Azari et al. (2006) reported essentially normal RNFL at 1.7 mm eccentricity from the disk by time domain OCT criteria. Our SD-OCT disk imaging studies showed either normal or *thickened* RNFL, not thinned, in both patients who could be ascertained. Of note, in PT3, custom RNFL scan measurements within 500 μm of the lamina cribrosa were necessary to reveal the thickening of the RNFL (see Supplemental Figure), which was otherwise not apparent to standard Cirrus disk SD-OCT scans, which are performed farther away from the disk. RNFL thickening was not an expected observation and is of uncertain etiology. Several explanations appear possible. The RNFL thickening may represent reactive gliosis within the retina secondary to the degenerative process. However, retinal lamination was well preserved in the areas where increased RNFL thickness was observed. Alternatively, the BBS1 gene product – and those of BBS genes in general – may be important for retinal ganglion cell (RGC) function too, and the RNFL thickening may be an expression of this putative role. This would be consistent not only with our previous observation of a clinical correlate between optic nerve appearance and visual acuity (Iannaccone et al., 1997) but also with the optic nerve dysfunction that we previously reported in BBS also by visual evoked potential (VEP) criteria (Forte et al., 1996). In addition, we have recently reported that auto-antibodies recognizing RGC or optic nerve antigens are a very common finding in patients with acquired autoimmune retinopathy (Adamus et al., 2011), and these findings correlate to presence of both changes in RNFL thickness and delayed VEPs. The development of secondary autoimmune phenomena in RP patients and animal models has been reported repeatedly in the past (Chant, Heckenlively, & Meyers-Elliott, 1985; Heckenlively, Jordan, & Aptsiauri, 1999; Radic et al., 2006; Reid, Forrester, & Campbell, 1986) and a role for autoimmunity is becoming increasingly well appreciated also in age-related macular degeneration (Iannaccone et al., 2012; Morohoshi, Ohbayashi, et al., 2012, Morohoshi, Patel, et al., 2012; Patel et al., 2005). We have observed auto-antibodies recognizing RGC or optic nerve antigens in various patients certainly affected with bona fide RP but complicated with clinically overt, steroid-responsive disk swelling and other inflammatory manifestations (Iannaccone & Adamus, 2012, unpublished observation). It is therefore possible that also the RNFL swelling seen in our BBS1 patients may have an autoimmune etiology, which may warrant further investigation. Lastly, we cannot exclude that, in the context of post-receptoral intraretinal remodeling and functional adaptations to the ongoing disease, the thickened RNFL may reflect also a compensatory mechanism at the RGC level. This may in part help explain why so many more BBS patients than non-syndromic RP patients develop non-recordable ERGs despite retaining well preserved field limits, like PT1, and as we reported previously (Iannaccone et al., 1996). Whatever the cause, the possibility of RGC/optic nerve compromise in BBS deserves further investigation, as it may have important implications for both pharmacological and gene therapy trials.

All of our patients demonstrated markedly reduced to non-recordable DA rod ERGs and electronegative ERGs. This is strikingly consistent with the observation by Azari et al. (2006). We have been able to demonstrate that two factors contribute jointly to the observed electronegativity: (1) exhaustion and impaired recycling of the visual pigments, leading to an excessive blunting of the rod-driven b-wave because of insufficient dark adaptation, and a progressive blunting of the b-wave response following serial bright flashes in the DA state, both phenomena that are similar to what is seen in patients with FA and RPA (Fishman et al., 2004; Iannaccone et al., 2007) – this observation is consistent with the depressed ERG sensitivity observed in M390R knock-in mice (Davis et al., 2007); (2) ON $\gg$ OFF bipolar cell response compromise – this is a novel finding, appeared to represent the main cause for ERG electronegativity, and its determinants are presently uncertain. In M390R knock-in mice, Davis et al. have reported rhodopsin mislocalization at the photoreceptor to bipolar cell synaptic pedicle (Davis et al., 2007). It is therefore possible that BBS1 patients experience ERG electronegativity for a proximal compromise of this synapse. Alternatively, the electronegativity may be due to intraretinal remodeling, as seen previously in RP (Cideciyan & Jacobson, 1993), though this phenomenon has not been reported in M390R knock-in mice (Davis et al., 2007), or to a distal photoreceptor-to-bipolar cell synaptic defect. Azari et al. (2006) also hypothesized that negative ERG waveforms represent a disease stage rather than a primary disease feature. Consistent also with this hypothesis, PT1 had initially markedly diminished and severely delayed ERGs, which progressed to an electronegative waveform 2 years later and ultimately became non-recordable. However, PT2 and PT3 exhibited electronegative ERGs at a relatively early disease stage. It will be of interest to see if, over time, PT2 and PT3 experience a change in this ERG feature, and whether additional studies on the M390R knock-in mice can help shed light on this novel finding.

In summary, our investigation confirms a number of previously documented features in BBS1 patients, and expands our understanding of the BBS1 ophthalmic phenotypic spectrum in M390R homozygotes by reporting novel findings which include electronegative LA ERG with ON $\gg$ OFF bipolar cell response compromise and increased RNFL thickness. In consideration of the high prevalence of the M390R mutation in the BBS population and the recent evidence that treatment with TUDCA prevented obesity and preserved ERG b-waves and ONL thickness in the aforementioned *Bbs1* knock-in M390R mice (Drack et al., 2011), increasing our understanding of BBS1 retinal, RPE and optic nerve pathology in patients homozygous for the M390R mutation is of great potential relevance to forthcoming treatment trial opportunities for patients affected by this otherwise lawful condition.

Acknowledgments

This investigation was supported by unrestricted grants from Research to Prevent Blindness, Inc., New York, NY, to the

Departments of Ophthalmology at the University of Tennessee Health Science Center and at the University of Iowa, by the Foundation Fighting Blindness, Owen Mills, MD, and by the Howard Hughes Medical Institute.

Appendix A. Supplementary material

Supplementary data associated with this article can be found, in the online version, at http://dx.doi.org/10.1016/j.visres.2012.08.005.

References

Adamus, G., Brown, L., Schiffman, J., & Iannaccone, A. (2011). Diversity in autoimmunity against retinal, neuronal, and axonal antigens in acquired neuro-retinopathy. *Journal of Ophthalmic Inflammation and Infection, 1*(3), 111–121.

Alexander, K. R., Barnes, C. S., & Fishman, G. A. (2001). High-frequency attenuation of the cone ERG and ON-response deficits in X-linked retinoschisis. *Investigative Ophthalmology and Visual Science, 42*(9), 2094–2101.

Anadoliiska, A., & Roussinov, D. (1993). Clinical aspects of renal involvement in Bardet–Biedl syndrome. *International Urology and Nephrology, 25*(5), 509–514.

Azari, A. A., Aleman, T. S., Cideciyan, A. V., Schwartz, S. B., Windsor, E. A., Sumaroka, A., et al. (2006). Retinal disease expression in Bardet–Biedl syndrome-1 (BBS1) is a spectrum from maculopathy to retina-wide degeneration. *Investigative Ophthalmology and Visual Science, 47*(11), 5004–5010.

Badano, J. L., Kim, J. C., Hoskins, B. E., Lewis, R. A., Ansley, S. J., Cutler, D. J., et al. (2003). Heterozygous mutations in BBS1, BBS2 and BBS6 have a potential epistatic effect on Bardet–Biedl patients with two mutations at a second BBS locus. *Human Molecular Genetics, 12*(14), 1651–1659.

Barnett, S., Reilly, S., Carr, L., Ojo, I., Beales, P. L., & Charman, T. (2002). Behavioural phenotype of Bardet–Biedl syndrome. *Journal of Medical Genetics, 39*(12), e76.

Beales, P. L., Warner, A. M., Hitman, G. A., Thakker, R., & Flinter, F. A. (1997). Bardet–Biedl syndrome: A molecular and phenotypic study of 18 families. *Journal of Medical Genetics, 34*(2), 92–98.

Berson, E. L., Rosner, B., Sandberg, M. A., Hayes, K. C., Nicholson, B. W., Weigel-DiFranco, C., et al. (1993). A randomized trial of vitamin A and vitamin E supplementation for retinitis pigmentosa. *Archives of Ophthalmology, 111*, 761–772.

Berson, E. L., Rosner, B., Sandberg, M. A., Weigel-DiFranco, C., Brockhurst, R. J., Hayes, K. C., et al. (2011). Clinical trial of lutein in patients with retinitis pigmentosa receiving vitamin A. *Archives of Ophthalmology, 128*(4), 403–411.

Berson, E. L., Rosner, B., Sandberg, M. A., Weigel-DiFranco, C., Moser, A., Brockhurst, R. J., et al. (2004a). Further evaluation of docosahexaenoic acid in patients with retinitis pigmentosa receiving vitamin A treatment: Subgroup analyses. *Archives of Ophthalmology, 122*(9), 1306–1314.

Berson, E. L., Rosner, B., Sandberg, M. A., Weigel-DiFranco, C., Moser, A., Brockhurst, R. J., et al. (2004b). Clinical trial of docosahexaenoic acid in patients with retinitis pigmentosa receiving vitamin A treatment. *Archives of Ophthalmology, 122*(9), 1297–1305.

Campo, R. V., & Aaberg, T. M. (1982). Ocular and systemic manifestations of the Bardet–Biedl syndrome. *American Journal of Ophthalmology, 94*, 750–756.

Chant, S. M., Heckenlively, J., & Meyers-Elliott, R. H. (1985). Autoimmunity in hereditary retinal degeneration. I. Basic studies. *British Journal of Ophthalmology, 69*(1), 19–24.

Churchill, D. N., McManamon, P., & Hurley, R. M. (1981). Renal disease – A sixth cardinal feature of the Laurence–Moon–Biedl syndrome. *Clinical Nephrology, 16*(3), 151–154.

Cideciyan, A., & Jacobson, S. (1993). Negative electroretinograms in retinitis pigmentosa. *Investigative Ophthalmology and Visual Science, 34*, 3253–3263.

Daniels, A. B., Sandberg, M. A., Chen, J., Weigel-Difranco, C., Hejtmancik, J. F., & Berson, E. L. (2012). Genotype–phenotype correlations in Bardet–Biedl syndrome. *Archives of Ophthalmology* (Epub ahead of print).

Davis, R. E., Swiderski, R. E., Rahmouni, K., Nishimura, D. Y., Mullins, R. F., Agassandian, K., et al. (2007). A knockin mouse model of the Bardet–Biedl syndrome 1 M390R mutation has cilia defects, ventriculomegaly, retinopathy, and obesity. *Proceedings of the National Academy of Sciences of the United States of America, 104*(49), 19422–19427.

Deveault, C., Billingsley, G., Duncan, J. L., Bin, J., Theal, R., Vincent, A., et al. (2011). BBS genotype–phenotype assessment of a multiethnic patient cohort calls for a revision of the disease definition. *Human Mutation, 32*(6), 610–619.

Drack, A. V., Dumitrescu, A. V., Bhattarai, S., Gratie, D., Stone, E. M., Mullins, R., et al. (2011). TUDCA slows retinal degeneration in two different mouse models of retinitis pigmentosa and prevents obesity in Bardet–Biedl syndrome type 1 mice. *Investigative Ophthalmology and Visual Science, 53*(1), 100–106.

Fishman, G. A., Roberts, M. F., Derlacki, D. J., Grimsby, J. L., Yamamoto, H., Sharon, D., et al. (2004). Novel mutations in the cellular retinaldehyde-binding protein gene (RLBP1) associated with retinitis punctata albescens: Evidence of interfamilial genetic heterogeneity and fundus changes in heterozygotes. *Archives of Ophthalmology, 122*(1), 70–75.

Forte, R., Iannaccone, A., De Propris, G., Del Beato, P., Rinaldi, R., Roncati, S., et al. (1996). The optic nerve in patients with the Laurence–Moon–Bardet–Biedl phenotype: A clinical and functional study. *Boll Oculist 75*(Suppl. 4), 115–124 (Italian).

Fulton, A. B., Hansen, R. M., & Glynn, R. J. (1993). Natural course of visual functions in the Bardet–Biedl syndrome. *Archives of Ophthalmology, 111*, 1500–1506.

Green, J. S., Parfrey, P. S., Harnett, J. D., Farid, N. R., Cramer, B. C., Johnson, G., et al. (1989). The cardinal manifestations of the Bardet–Biedl syndrome, a form of Laurence–Moon–Biedl syndrome. *New England Journal of Medicine, 321*, 1002–1009.

Grover, S., Fishman, G. A., Gilbert, L. D., & Anderson, R. J. (1997). Reproducibility of visual acuity measurements in patients with retinitis pigmentosa. *Retina, 17*, 33–37.

Heckenlively, J. R., Jordan, B. L., & Aptsiauri, N. (1999). Association of antiretinal antibodies and cystoid macular edema in patients with retinitis pigmentosa. *American Journal of Ophthalmology, 127*(5), 565–573.

Hurley, R. M., Dery, P., Nogrady, M. B., & Drummond, K. N. (1975). The renal lesion of the Laurence–Moon–Biedl syndrome. *Journal of Pediatrics, 87*(2), 206–209.

Iannaccone, A. (2005). The genetics of hereditary retinopathies and optic neuropathies. *Comprehensive Ophthalmology Update, 5*, 39–62.

Iannaccone, A., De Propris, G., Roncati, S., Rispoli, E., Del Porto, G., & Pannarale, M. R. (1997). The ocular phenotype of the Bardet–Biedl syndrome. Comparison to non-syndromic retinitis pigmentosa. *Ophthalmic Genetics, 18*, 13–26.

Iannaccone, A., Falsini, B., Haider, N., Del Porto, G., Stone, E. M., & Sheffield, V. C. (1999). Bardet–Biedl syndrome. Phenotypic characteristics associated with the BBS4 locus. In J. G. Hollyfield, M. M. La Vail, & R. E. Anderson (Eds.), *Retinal degenerative diseases and experimental therapy* (pp. 187–199). New York: Kluwer Academic/Plenum Press.

Iannaccone, A., Kritchevsky, S. B., Ciccarelli, M. L., Tedesco, S. A., Macaluso, C., Kimberling, W. J., et al. (2004). Kinetics of visual field loss in Usher syndrome Type II. *Investigative Ophthalmology and Visual Science, 45*(3), 784–792.

Iannaccone, A., Man, D., Waseem, N., Jennings, B. J., Ganapathiraju, M., Gallaher, K., et al. (2006). Retinitis pigmentosa associated with rhodopsin mutations: Correlation between phenotypic variability and molecular effects. *Vision Research, 46*(27), 4556–4567.

Iannaccone, A., Mykytyn, K., Persico, A. M., Searby, C. C., Baldi, A., Jablonski, M. M., et al. (2005). Clinical evidence of decreased olfaction in Bardet–Biedl syndrome caused by a deletion in the BBS4 gene. *American Journal of Medical Genetics Part A, 132*(4), 343–346.

Iannaccone, A., Neeli, I., Krishnamurthy, P., Lenchik, N. I., Wan, H., Gerling, I. C., et al. (2012). Autoimmunity in age-related macular degeneration: A possible role player in disease development and progression. *Advances in Experimental Medicine and Biology, 723*, 11–16.

Iannaccone, A., Othman, M. I., Cantrell, A. D., Jennings, B. J., Branham, K., & Swaroop, A. (2008). Retinal phenotype of an X-linked pseudo-Usher syndrome in association with the G173R mutation in the RPGR gene. *Advances in Experimental Medicine and Biology, 613*, 221–227.

Iannaccone, A., Tedesco, S. A., Gallaher, K. T., Yamamoto, H., Charles, S., & Dryja, T. P. (2007). Fundus albipunctatus in a 6-year old girl due to compound heterozygous mutations in the RDH5 gene. *Documenta Ophthalmologica, 115*(2), 111–116.

Iannaccone, A., Vingolo, E. M., Rispoli, E., De Propris, G., Tanzilli, P., & Pannarale, M. R. (1996). Electroretinographic alterations in the Laurence–Moon–Bardet–Biedl phenotype. *Acta Ophthalmologica Scandinavica, 74*, 8–13.

Jacobson, S. G., Borruat, F., & Apathy, P. P. (1990). Patterns of rod and cone dysfunction in Bardet–Biedl syndrome. *American Journal of Ophthalmology, 109*(June), 676–688.

Katsanis, N., Ansley, S. J., Badano, J. L., Eichers, E. R., Lewis, R. A., Hoskins, B. E., et al. (2001). Triallelic inheritance in Bardet–Biedl syndrome, a Mendelian recessive disorder. *Science, 293*(5538), 2256–2259.

Khan, N. W., Jamison, J. A., Kemp, J. A., & Sieving, P. A. (2001). Analysis of photoreceptor function and inner retinal activity in juvenile X-linked retinoschisis. *Vision Research, 41*, 3931–3942.

Leys, M. J., Schreiner, L. A., Hansen, R. M., Mayer, D. L., & Fulton, A. B. (1988). Visual acuities and dark-adapted thresholds of children with Bardet–Biedl syndrome. *American Journal of Ophthalmology, 106*(November), 561–569.

Loktev, A. V., Zhang, Q., Beck, J. S., Searby, C. C., Scheetz, T. E., Bazan, J. F., et al. (2008). A BBSome subunit links ciliogenesis, microtubule stability, and acetylation. *Developmental Cell, 15*(6), 854–865.

Morohoshi, K., Ohbayashi, M., Patel, N., Chong, V., Bird, A. C., & Ono, S. J. (2012). Identification of anti-retinal antibodies in patients with age-related macular degeneration. *Experimental and Molecular Pathology, 93*(2), 193–199.

Morohoshi, K., Patel, N., Ohbayashi, M., Chong, V., Grossniklaus, H. E., Bird, A. C., et al. (2012). Serum autoantibody biomarkers for age-related macular degeneration and possible regulators of neovascularization. *Experimental and Molecular Pathology, 92*(1), 64–73.

Mykytyn, K., Mullins, R. F., Andrews, M., Chiang, A. P., Swiderski, R. E., Yang, B., et al. (2004). Bardet–Biedl syndrome type 4 (BBS4)-null mice implicate Bbs4 in flagella formation but not global cilia assembly. *Proceedings of the National Academy of Sciences of the United States of America, 101*(23), 8664–8669.

Mykytyn, K., Nishimura, D. Y., Searby, C. C., Beck, G., Bugge, K., Streb, L. M., et al. (2003). Evaluation of complex inheritance involving the most common Bardet–Biedl syndrome locus (BBS1). *American Journal of Human Genetics, 72*(2), 429–437.

Mykytyn, K., Nishimura, D. Y., Searby, C. C., Shastri, M., Yen, H. J., Beck, J. S., et al. (2002). Identification of the gene (BBS1) most commonly involved in Bardet–Biedl syndrome, a complex human obesity syndrome. *Nature Genetics, 31*(4), 435–438.

Mykytyn, K., & Sheffield, V. C. (2004). Establishing a connection between cilia and Bardet–Biedl syndrome. *Trends in Molecular Medicine, 10*(3), 106–109.

O'Dea, D., Parfrey, P. S., Harnett, J. D., Hefferton, D., Cramer, B. C., & Green, J. (1996). The importance of renal impairment in the natural history of Bardet–Biedl syndrome. *American Journal of Kidney Diseases, 27*(6), 776–783.

Ozer, G., Yuksel, B., Suleymanova, D., Alhan, E., Demircan, N., & Onenli, N. (1995). Clinical features of Bardet–Biedl syndrome. *Acta Paediatrica Japonica, 37*, 233–236.

Patel, N., Ohbayashi, M., Nugent, A. K., Ramchand, K., Toda, M., Chau, K. Y., et al. (2005). Circulating anti-retinal antibodies as immune markers in age-related macular degeneration. *Immunology, 115*(3), 422–430.

Perez Perez, A. J., & Barrio, C. (1998). Kidney disease in Bardet–Biedl syndrome. *Nephrology, Dialysis, Transplantation, 13*, 510–511.

Pretorius, P. R., Aldahmesh, M. A., Alkuraya, F. S., Sheffield, V. C., & Slusarski, D. C. (2011). Functional analysis of BBS3 A89V that results in non-syndromic retinal degeneration. *Human Molecular Genetics, 20*(8), 1625–1632.

Pretorius, P. R., Baye, L. M., Nishimura, D. Y., Searby, C. C., Bugge, K., Yang, B., et al. (2010). Identification and functional analysis of the vision-specific BBS3 (ARL6) long isoform. *PLoS Genetics, 6*(3), e1000884.

Radic, M. Z., Shah, K., Zhang, W., Lu, Q., Lemke, G., & Hilliard, G. M. (2006). Heterogeneous nuclear ribonucleoprotein P2 is an autoantibody target in mice deficient for Mer, Axl, and Tyro3 receptor tyrosine kinases. *Journal of Immunology, 176*(1), 68–74.

Reid, D. M., Forrester, J. V., & Campbell, A. M. (1986). Monoclonal autoantibodies from rats with inherited retinal dystrophy. *Journal of Clinical and Laboratory Immunology, 21*(4), 165–168.

Riise, R., Andreasson, S., Wright, A. F., & Tornqvist, K. (1996). Ocular findings in the Laurence–Moon–Bardet–Beidl syndrome. *Acta Ophthalmologica Scandinavica, 74*, 612–617.

Seo, S., Baye, L. M., Schulz, N. P., Beck, J. S., Zhang, Q., Slusarski, D. C., et al. (2010). BBS6, BBS10, and BBS12 form a complex with CCT/TRiC family chaperonins and mediate BBSome assembly. *Proceedings of the National Academy of Sciences of the United States of America, 107*(4), 1488–1493.

Shah, A. S., Farmen, S. L., Moninger, T. O., Businga, T. R., Andrews, M. P., Bugge, K., et al. (2008). Loss of Bardet–Biedl syndrome proteins alters the morphology and function of motile cilia in airway epithelia. *Proceedings of the National Academy of Sciences of the United States of America, 105*(9), 3380–3385.

Sieving, P. A. (1993). Photopic ON- and OFF-pathway abnormalities in retinal dystrophies. *Transactions of the American Ophthalmological Society, LXXXXI*, 701–773.

Sieving, P. A., Murayama, K., & Naarendorp, F. (1994). Push–pull model of the primate photopic electroretinogram: A role for hyperpolarizing neurons in shaping the b-wave. *Visual Neuroscience, 11*, 519–532.

Simons, D. L., Boye, S. L., Hauswirth, W. W., & Wu, S. M. (2011). Gene therapy prevents photoreceptor death and preserves retinal function in a Bardet–Biedl syndrome mouse model. *Proceedings of the National Academy of Sciences of the United States of America, 108*(15), 6276–6281.

Spaide, R. F., Koizumi, H., & Pozzoni, M. C. (2008). Enhanced depth imaging spectral-domain optical coherence tomography. *American Journal of Ophthalmology, 146*(4), 496–500.

Swiderski, R. E., Nishimura, D. Y., Mullins, R. F., Olvera, M. A., Ross, J. L., Huang, J., et al. (2007). Gene expression analysis of photoreceptor cell loss in bbs4-knockout mice reveals an early stress gene response and photoreceptor cell damage. *Investigative Ophthalmology and Visual Science, 48*(7), 3329–3340.

Zhang, Q., Nishimura, D., Seo, S., Vogel, T., Morgan, D. A., Searby, C., et al. (2012). Bardet–Biedl syndrome 3 (Bbs3) knockout mouse model reveals common BBS-associated phenotypes and Bbs3 unique phenotypes. *Proceedings of the National Academy of Sciences of the United States of America, 108*(51), 20678–20683.

Zhang, Q., Yu, D., Seo, S., Stone, E. M., & Sheffield, V. C. (2012). Intrinsic protein–protein interaction mediated and chaperonin assisted sequential assembly of a stable Bardet Biedl syndome protein complex, the BBSome. *Journal of Biological Chemistry, 287*(24), 20625–20635.